Langmuir Article

pubs.acs.org/Langmuir
© 2010 American Chemical Society

Genetically Engineered Liquid-Crystalline Viral Films for Directing Neural Cell Growth

Woo-Jae Chung, Anna Merzlyak, So Young Yoo, and Seung-Wuk Lee*

Department of Bioengineering, University of California, Berkeley, California, and Physical Biosciences Division, Lawrence Berkeley National Laboratory, Berkeley Nanoscience and Nanoengineering Institute, Berkeley, California 94720

Received January 16, 2010. Revised Manuscript Received April 13, 2010

Designing biomimetic matrices with precisely controlled structural organization that provides biochemical and physical cues to regulate cell behavior is critical for the development of tissue-regenerating materials. We have developed novel liquid-crystalline film matrices made from genetically engineered M13 bacteriophages (viruses) that exhibit the ability to control and guide cell behavior for tissue-regenerating applications. To facilitate adhesion between the viruses and cells, 2700 copies of the M13 major coat protein were genetically engineered to display integrin-binding peptides (RGD). The resulting nanofiber-like viruses displaying RGD motifs were biocompatible with neuronal cells and could be self-assembled to form long-range-ordered liquid-crystalline matrices by a simple shearing method. The resulting aligned structures were able to dictate the direction of cell growth. Future use of these virus-based materials for regenerating target tissues *in vivo* would provide great opportunities for various tissue therapies.

Introduction

Tissue engineering aims to regenerate and replace damaged or diseased tissues using tissue constructs created ex vivo or in vivo.[1,2] Thus, the ultimate purpose of tissue-engineering scaffolds is to provide a synthetic microenvironment that can support the growth of target cells and regulate their fates and functions. The design of tissue-engineering materials takes into consideration the in vivo cellular environment where cells are in close contact with other cells as well as the extracellular matrix (ECM). In nature, ECM mainly consists of an interconnected network of fibrous protein matrices that form self-organized structures to provide chemical and mechanical cues for guiding cell behavior and growth.[3] Various fibrous network scaffold structures have been prepared by utilizing electrospinning,[4,5] peptide self-assembly,[6,7] and polymer phase separation.[8,9] These fibrous morphologies closely resemble the structures of native ECM and may be useful in regenerating damaged tissues or organs.

Recently, various viral particles have been used to construct functional nanoscale materials and devices (e.g., electronic components and energy storage materials)[10,11] and for biomedical purposes.[12−17] In particular, filamentous M13 bacteriophages (viruses) possess several attributes that mimic fibrous self-organized tissue-engineering scaffolds.[12,13] A high density of peptide signaling motifs can be displayed on viral coat proteins through genetic engineering. A large quantity of identical phage building blocks can be easily prepared through amplification using a bacterial host (*E. coli*). Because of the monodispersity and high aspect ratio of the phage, self-assembled phage structures can easily be fabricated without microfabrication techniques by controlling the concentration of the suspension or external force fields. Because prokaryotic phages are ignored by eukaryotic cell systems, bacteriophages are known to cause few harmful effects on animal cells, as shown in previous studies.[14,15] Therefore, phage-based therapies have been extensively studied for potential medical applications including drug/gene delivery, in vivo functional peptide discovery, and antibiotic therapies.[16] The incorporation of cell-binding motifs into the phage particles using a chemical approach has also been demonstrated to show the directional growth of fibroblast cells on their uniformly aligned structures.[13]

Previously, we have demonstrated that genetically modified M13 phages can be assembled to form 3D fiber matrices that encapsulate cells and successfully guide the cellular growth process inside the scaffold.[12] The results indicated that the genetically modified phages can be used as versatile building blocks to construct well-defined 3D tissue-engineering scaffolds. Here, we report on the self-assembly of genetically engineered M13 phages into liquid-crystalline viral films using a facile shearing method. The resulting viral liquid-crystalline films exhibited centimeter-scale long-range-ordered 2D topographies and enabled us to dictate the directional growth of hippocampal

*To whom correspondence should be addressed. E-mail: leesw@berkeley.edu.

(1) Langer, R.; Vacanti, J. P. *Science* **1993**, *260*, 920−926.
(2) Stevens, M. M.; Marini, R. P.; Schaefer, D.; Aronson, J.; Langer, R.; Shastri, V. P. *Proc. Natl. Acad. Sci. U.S.A.* **2005**, *102*, 11450–11455.
(3) Andrew, C. A. W.; Evelyn, K. F. Y.; Liao, I. C.; Catherine Le, V.; Kam, W. L. *J. Biomed. Mater. Res., Part A* **2004**, *71A*, 586–595.
(4) Ma, Z.; Kotaki, M.; Inai, R.; Ramakrishna, S. *Tissue Eng.* **2005**, *11*, 101–109.
(5) Yang, F.; Murugan, R.; Wang, S.; Ramakrishna, S. *Biomaterials* **2005**, *26*, 2603–2610.
(6) Silva, G. A.; Czeisler, C.; Niece, K. L.; Beniash, E.; Harrington, D. A.; Kessler, J. A.; Stupp, S. I. *Science* **2004**, *303*, 1352–1355.
(7) Zhao, X.; Zhang, S. *Trends Biotechnol.* **2004**, *22*, 470–476.
(8) Ma, P. X. *Adv. Drug Delivery Rev.* **2008**, *60*, 184–198.
(9) Guan, J.; Fujimoto, K. L.; Sacks, M. S.; Wagner, W. R. *Biomaterials* **2005**, *26*, 3961–3971.
(10) Lee, S.-W.; Mao, C.; Flynn, C. E.; Belcher, A. M. *Science* **2002**, *296*, 892–895.
(11) Nam, K. T.; Kim, D.-W.; Yoo, P. J.; Chiang, C.-Y.; Meethong, N.; Hammond, P. T.; Chiang, Y.-M.; Belcher, A. M. *Science* **2006**, *312*, 885–888.
(12) Merzlyak, A.; Indrakanti, S.; Lee, S.-W. *Nano Lett.* **2009**, *9*, 846–852.
(13) Rong, J.; Lee, L. A.; Li, K.; Harp, B.; Mello, C. M.; Niu, Z.; Wang, Q. *Chem. Commun.* **2008**, *41*, 5185–5187.
(14) Li, Z.; Koch, H.; Dübelc, S. *J. Mol. Microbiol. Biotechnol.* **2003**, *6*, 57–66.
(15) Smith, G. P.; Petrenko, V. A. *Chem. Rev.* **1997**, *97*, 391−410.
(16) Clark, J. R.; March, J. B. *Trends Biotechnol.* **2006**, *24*, 212–218.
(17) Souza, G. R.; Christianson, D. R.; Staquicini, F. I.; Ozawa, M. G.; Snyder, E. Y.; Sidman, R. L.; Miller, J. H.; Arap, W.; Pasqualini, R. *Proc. Natl. Acad. Sci. U.S.A.* **2006**, *103*, 1215–1220.

neural progenitor cells (NPCs). Additionally, the remarkable specific effect of the RGD-engineered phage films on cell adhesion and the cellular growth is shown in the present study. In addition, we found that our genetically modified films could be applied to other cell types including fibroblast and preosteoblast cells.

Experimental Section

Genetic Engineering of the M13 Bacteriophage. The M13 bacteriophage was engineered to display specific peptide motifs on its major coat protein (pVIII) by using a partial library cloning approach. An octapeptide was inserted at the N-terminus of the pVIII and positioned between the first and the fifth amino acids of wild-type pVIII, replacing residues 2−4 (Ala-**Glu-Gly-Asp**-Asp to Ala-(**insert**)-Asp) as previously reported.[18] A sequence-specific RGE phage was engineered via the same cloning method to serve as a control for the RGD-phage. The primer was designed to match the RGD-phage exactly but with glutamic acid substituted for aspartic acid. The forward primer used to construct the RGE phage was 5′ ATATATCTG CAG *ACTCGGGACGTGGT-GAAACCGAA* GAT CCC GCAAAAGCGGCC-TTTAACT CCC 3′, with the resulting sequence of A*DSG**RGE**TE*DP. The constructed phages were amplified using bacterial cultures and purified through the standard polyethylene glycol precipitation method. The phage solution was further purified by filtration through 0.45-μm-pore-size membranes. To verify phage stability, DNA sequences were confirmed at each step of the amplification.

Phage Film Fabrication. Glass slide substrates were placed in piranha solution for 10 min (1:4 H_2O_2/H_2SO_4), thoroughly rinsed with DI water, and dried in a stream of nitrogen. Then, the substrates were treated with 1% (v/v) 3-aminopropyl triethoxysilane (APTS) solution in EtOH. Subsequently, the substrates were rinsed with EtOH to remove excess silane and annealed at 100 °C for 10 min. For the preparation of isotropic phage films, a phage solution (50 μL of 10^{12} viruses/mL) in PBS was spread onto the APTS-treated glass surface (1 × 1 cm^2) and allowed to dry overnight at 37 °C in a humidified incubator. For the preparation of aligned phage films with anisotropic topography, a droplet (5 μL) of the phage solution (10−30 mg/mL) was placed on one edge of the APTS-treated glass substrate (1 × 2.5 cm^2) and dragged using a glass slide parallel to the long axis of the glass substrate to apply a shear force in a single direction. The film samples were dried overnight at room temperature and rinsed gently with PBS prior to cell culture experiments.

Microscopy Analysis of Phage Solution and Phage Film. Polarized optical microscopy images of the liquid-crystalline phases of the phage solutions were taken using an X71 Olympus Microscope (Olympus Inc., Japan) equipped with two polarized optical filters. The scanning microscopy image of the phage was taken using a Hitachi environmental scanning electron microscope (SEM, S-4300 SE/N, Hitachi, Hitachi Inc., Japan) after the sheared phage film was critically point dried (using a Tousimis AutoSamdri 815 critical point dryer, Electron Microscopy Laboratory, University of California, Berkeley, Berkeley, CA). The topographic images of the phage films were acquired in air using AFM (MFP-3D AFM, Asylum Research, Santa Barbara, CA) operating in tapping mode with a silicon cantilever (AC240TS, Olympus, Tokyo, Japan). The typical scan size was 20 × 20 μm^2, and the scan rate was 0.5 Hz. The rms roughness of the phage film surface was measured using Igor Pro MFP-3D software (Asylum Research, Santa Barbara, CA). Height difference profiles were determined from line profiles traced perpendicularly through the features of interest on the phage films.

Cell Culture on a Phage Film. Hippocampal neural progenitor cells (NPCs) isolated from adult rats (a gift from Prof. David Schaffer, University of California, Berkeley, CA) were used at passage numbers 40−45 and seeded at a density of ~3 × 10^4 cells/cm^2 on the phage films. The cells were grown in DMEM/F12 media with N-2 supplement (Invitrogen, Carlsbad, CA) at 37 °C with 5% CO_2. For cell proliferation, the media were supplemented with 20 ng/mL bFGF (Peprotech, Rocky Hill, NJ); for cell differentiation, the media were supplemented with 1 μM retinoic acid and 5 μM forskolin (Biomol, Plymouth Meeting, PA).[19]

Fluorescence Microscopy Imaging of Cells Cultured on a Phage Film. Cells cultured on the phage films were fixed in 4% paraformaldehyde for 15 min and then blocked with a solution of 0.3% Triton X-100 and 5% normal goat serum in PBS for 30 min. To stain the NPCs, primary antibodies for identifying cell markers and for the M13 bacteriophage were incubated with the cells overnight at 4 °C. The primary antibodies used in this investigation were mouse anti-β-III-tubulin antibody (TUBB3) (1:400, Sigma Aldrich, St. Louis, MO), mouse anti-nestin antibody (1:1000, BD Biosciences, San Jose, CA), and rabbit anti-fd antibody (1:500, Sigma Aldrich, St. Louis, MO). Secondary goat Alexa flourochrome-conjugated antibodies (Molecular Probes, Eugene, OR) were used in a dilution of 1:250 to visualize the markers and were incubated with the cells for 2 h at room temperature. A 300 nM DAPI (Molecular Probes, Eugene, OR) solution in PBS was used as the nucleus counterstain for all samples. The fluorescence images were collected using an IX71 fluorescence microscope (Olympus, Tokyo, Japan).

Spatial Distribution Analysis of Cells Cultured on a Phage Film. The spatial distribution analysis of the cells on various engineered phage and control surfaces was performed using NIH ImageJ and R (http://www.R-project.org) software packages. The images of cell nuclei were initially processed with ImageJ to be represented by particles, and their centroid coordinates were determined. This data was then imported into R for nearest-neighbor analysis using the SpatStat module.[20] The angle and elongation of cells were identified for 100−200 cells on each phage film using ImageJ.

Results and Discussion

To develop novel phage-based tissue-engineering matrices, we genetically engineered M13 phages to display integrin-binding peptide RGD and a control peptide RGE at the *N*-terminus of their major coat protein (pVIII) (Figure 1). Approximately 2700 copies of RGD peptide were displayed on each virus and packed tightly around the phage body with 5-fold symmetry. The RGD-modified proteins represent 99% of the viral coat surface and were displayed at a high density of 1.5×10^{13} epitopes/cm^2.[12] The peptide array is uniformly spaced at 2.7 nm in the axial direction and 2 nm in the lateral direction. The wild-type M13KE phage, displaying no peptide insert, was used as a nonspecific control. Large quantities of the RGD- and RGE-phages could be produced through bacterial amplification (~100 mg/L).

To investigate the efficacy of the RGD-phage as a tissue-engineering material, we prepared drop-cast films of the phage on glass substrates and characterized their effects on neural progenitor cells (NPCs). We monitored NPC viability on the RGD-phage film, control phage films (RGE and wild-type), and a laminin-coated surface (positive control, see Supporting Information) for 4 days in DMEM/F12 (1:1) media (1% N-2). NPCs on the RGD-phage film were evenly distributed in a manner similar to that observed on the laminin-coated surface (Figure 2a,c). In contrast, RGE and wild-type-phage films induced cells to form aggregates containing cell cluster morphology (Figure 2b and Supporting Information Figure S1a). These results concurred with previous findings that NPCs aggregate into neurosphere clusters when

(18) Merzlyak, A.; Lee, S.-W. *Bioconjugate Chem.* **2009**, *20*, 2300–2310.

(19) Palmer, T. D.; Ray, J.; Gage, F. H. *Mol. Cell. Neurosci.* **1995**, *6*, 474–486.

(20) Baddeley, A.; Turner, R. *J. Stat. Software* **2005**, *12*, 1–42.

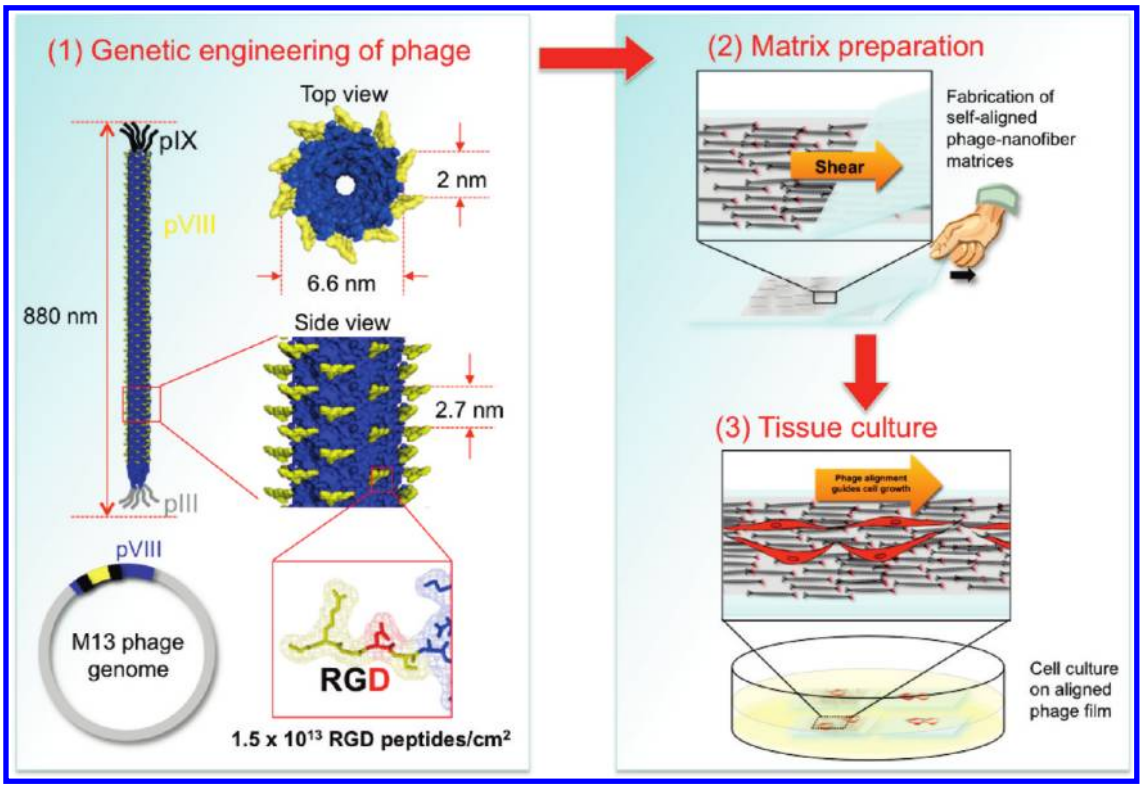

Figure 1. Schematic illustration of genetically engineered M13 phages and their self-assembly into a functional phage film for tissue-engineering scaffolds. The M13 phage was genetically engineered to display integrin-binding motif RGD on every copy of pVIII. The 2D liquid-crystalline phage film was constructed by shearing M13 phage solution on the substrate to align the phage for directing cell growth.

grown on poorly adhesive surfaces.[21] The number of NPCs attached on the RGD-phage film was found to be similar to that on the laminin-coated substrate (Figure 2d). However, the control RGE phage film, which differed from the RGD-phage film only in one additional methylene group in its glutamate, exhibited a significant decrease in the number of attached cells (~37%); the wild-type-phage film (displaying no peptide insert) showed a drastic decrease in cell attachment (~83%) (Figure 2d). We quantified the differences in the spatial distribution of cells on each phage film using nearest-neighbor analysis.[22] The spatial distribution of cells grown on laminin was most similar to the theoretically "independent" distribution, which means that the substrate provided the most cell-adhesive surface in a way in which cell attachment on the surface took place independently from that of the neighboring cells. Among the cells grown on phage films, the cells on the RGD-phage film have shown the closest spatial distribution to the cells grown on laminin. Cells grown on RGE- and wild-type-phage films exhibited spatial distributions that deviated significantly more from the independent distribution and approached the "cluster" distribution (Figure 2e). This indicates that the control phage films provided poorly cell-adhesive surfaces leading to more cell clustering. The cell spreading and the spatial distribution of NPCs on the RGD-phage film demonstrated that the RGD adhesive ligands displayed on the film were fully available for cell attachment on the surface.

The interaction of the RGD motif with the cells was also evident when NPCs were grown in neural differentiation media. NPCs on laminin and RGD-, RGE- and wild-type-phage films differentiated into a neuronal lineage, as verified by their morphology and expression of neuronal β-III-tubulin, which was confirmed with a specific antibody (TUBB3) as a marker for neuron-specific differentiation (Figure 2f−h and Supporting Information Figure S1b). Compared to cells grown on the control phage films (RGE and wild-type), differentiated NPCs on the RGD-phage film exhibited a relatively more even cell distribution although they exhibited more aggregated morphology comparing to those on the laminin (Supporting InformationFigure S2). It is interesting that when we performed immunofluorescent staining of the phage on each film (Supporting Information Figure S3), fluorescence intensity plots revealed higher concentrations of phage antibodies at cell locations on the RGD-phage films. In contrast, decreased fluorescence intensities of phage antibody were observed at cell locations on the RGE- and wild-type-phage films. We believe that these variations were also due to the enhanced cell interactions with the RGD-phages. Previously, phages displaying RGD-containing peptides have been demonstrated to be internalized by mammalian cells via integrin-mediated endocytosis.[23−25] In addition, we recently found that our genetically engineered RGD-phages have enhanced internalization capabilities into HeLa cells comparing to that of the control RGE- and wild-type-phages (data not shown). Therefore, we believe that more concentrated phage particles within the cells resulted from the cell internalization of RGD-phages from the phage films. On the basis of our observation, we confirmed that the RGD peptide motifs conferred greater cell specificity to the RGD-phage films.

(21) Krishanu, S.; Elizabeth, F. I.; Julia, K.; David, V. S.; Kevin, E. H. *J. Biomed. Mater. Res., Part A* **2007**, *81A*, 240–249.
(22) Clark, P. J.; Evans, F. C. *Ecology* **1954**, *35*, 445–453.
(23) Hart, S. L.; Knight, A. M.; Harbottle, R. P.; Mistry, A.; Hunger, H. D.; Cutler, D. F.; Williamson, R.; Coutelle, C. *J. Biol. Chem.* **1994**, *269*, 12468–12474.
(24) Pasqualini, R.; Koivunen, E.; Ruoslahti, E. *Nat. Biotechnol.* **1997**, *15*, 542–546.
(25) Ivanenkov, V. V.; Felici, F.; Menon, A. G. *Biochim. Biophys. Acta* **1999**, *1448*, 450–462.

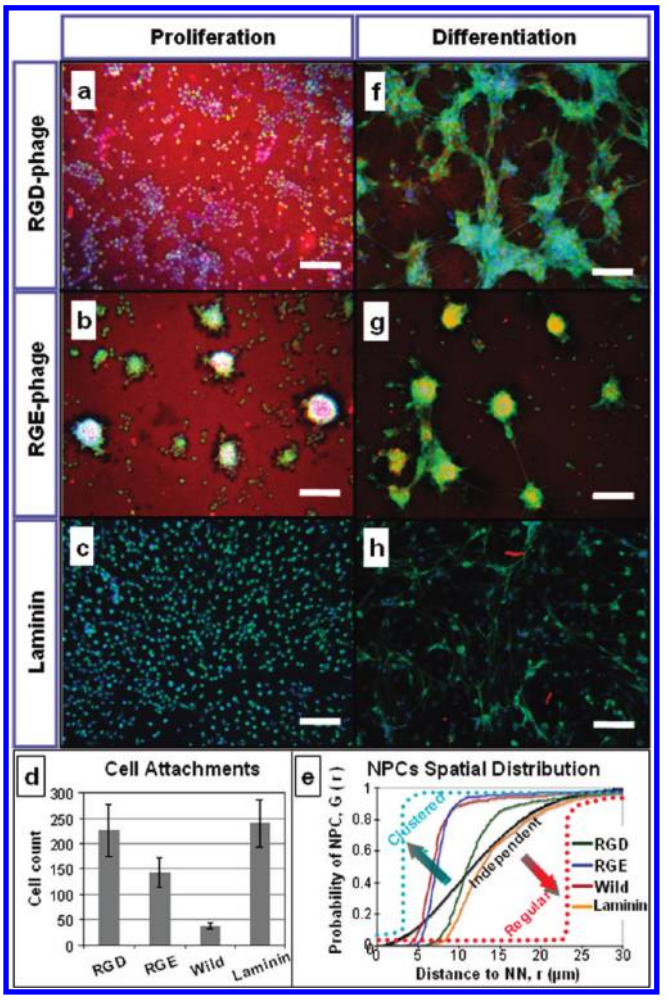

Figure 2. Specific effects of RGD-phage films on neural progenitor cell (NPC) growth patterns. Composite immunofluorescent staining images of proliferated NPCs (on day 4) on (a, b) RGD-phage films and (c) a laminin-coated substrate, stained for nestin (green) and phage (red) and counterstained with DAPI (blue). (d) Counting adhered NPCs on a phage film after 4 days of culturing. (e) Plot of the spatial distribution of NPCs on phage-coated substrates. The spacing of cells ranged from independent to clustered, or regular from nearest-neighbor analysis. Composite immunofluorescent staining images of NPCs in differentiation media grown (on day 8) on top of (f, g) RGD-phage films and (h) a laminin-coated substrate, stained for β-III-tubulin (green) and phage (red) and counterstained with DAPI (blue). Scale bars indicate 100 μm.

To examine the ability of the phage to self-assemble into a matrix with anisotropic topography that is able to guide the direction of cell growth, we prepared liquid-crystalline phage films with long-range orientation by applying a shearing force to the phage solution. Liquid-crystalline solutions of phage (10−30 mg/mL) were examined in a capillary using polarized optical microscopy (Figure 3a and Figure S4a) and were found to possess a nematic liquid-crystalline pattern. A droplet of the solution was then placed on the surface of an amino silane-treated glass substrate, and a shearing force parallel to the long axis of the glass substrate was applied using a clean glass slide (Figure 1). The sheared phage films were critical point dried, and scanning electron microscopy was used to determine that the long axis of all of the phage bundles were aligned along the direction of shear (Figure 3b). Atomic force micrographs also showed that the films possessed long-range nematically ordered surface morphologies

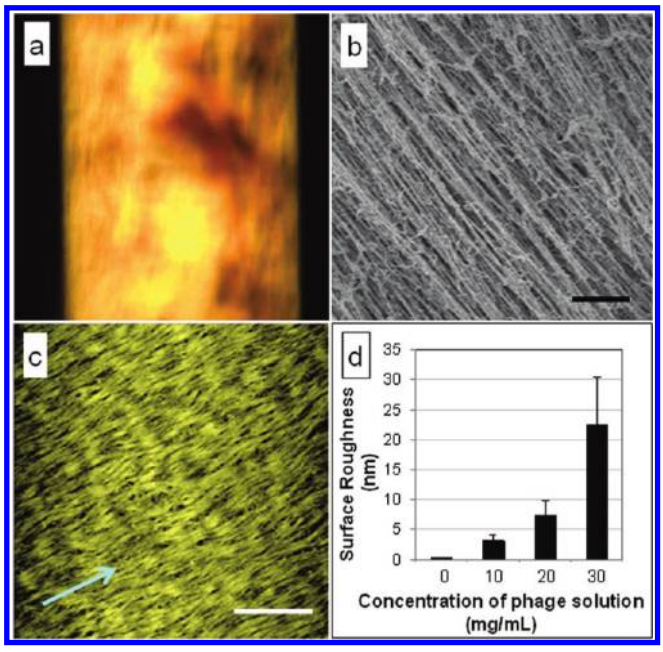

Figure 3. Structural analysis of the liquid-crystalline phage tissue matrices. (a) Polarized optical micrographs of the liquid-crystalline solution of phage (20 mg/mL). (b) Scanning electron micrograph of the sheared phage film after critical-point drying. (c) Atomic force micrograph showing long-range-ordered liquid-crystalline viral films (20 mg/mL). (d) Correlation between surface roughness and the concentration of the phage solution. Scale bars indicate (b) 1 μm and (c) 5 μm.

with roughness that could be controlled by the initial concentration of the phage solutions (Figure 3c,d). The sheared phage films revealed corrugated surface morphology with periodic, strongly anisotropic grooves and ridges aligned parallel to the direction of shear. However, nonsheared drop-cast phage films exhibited a surface morphology of randomly oriented phage bundles (Supporting Information Figure S4b). In the sheared films, the phage particles assembled into fiber bundles with directionally aligned submicrometer topography. The amplitude and roughness of the topography were tunable by varying the initial phage concentrations (rms = 3.1 ± 0.6 nm (10 mg/mL), 7.4 ± 1.8 nm (20 mg/mL), and 22.4 ± 5.3 nm (30 mg/mL)). The diameters of the fiber bundles were also shown to be tunable (20−900 nm) (Figure 3c and Supporting Information Figure S4c,d). Therefore, controllable nanometer-scale topographic features can be constructed on the sheared phage films to direct cell growth and encourage integrin-mediated polarization.

The ability of the sheared phage films to direct NPC growth was studied. NPCs were cultured on each of the aligned phage films (RGD, RGE, and wild-type) in tissue culture plates (3×10^4 cells/cm^2). Under both proliferation and differentiation conditions, NPCs on the sheared RGD-phage films showed growth patterns along the direction of phage alignment (Figure 4). Four hours after cell seeding in a proliferation medium, only NPCs on the aligned RGD-phage film were observed to extend their filamentous cytoskeleton (Supporting Information Figure S5), indicating that the integrin binding motif played an essential role in cell adhesion and spreading (elongation = 3.0 ± 1.6). Over 80% of the elongated NPCs were aligned within a ±20° angle of the phage fibers, indicating that the anisotropic topography of RGD-phage film strongly contributed to the orientation of NPC growth (Figure 4i). Twenty-four hours after seeding, NPCs on the aligned RGD-phage film were found to have proliferated along

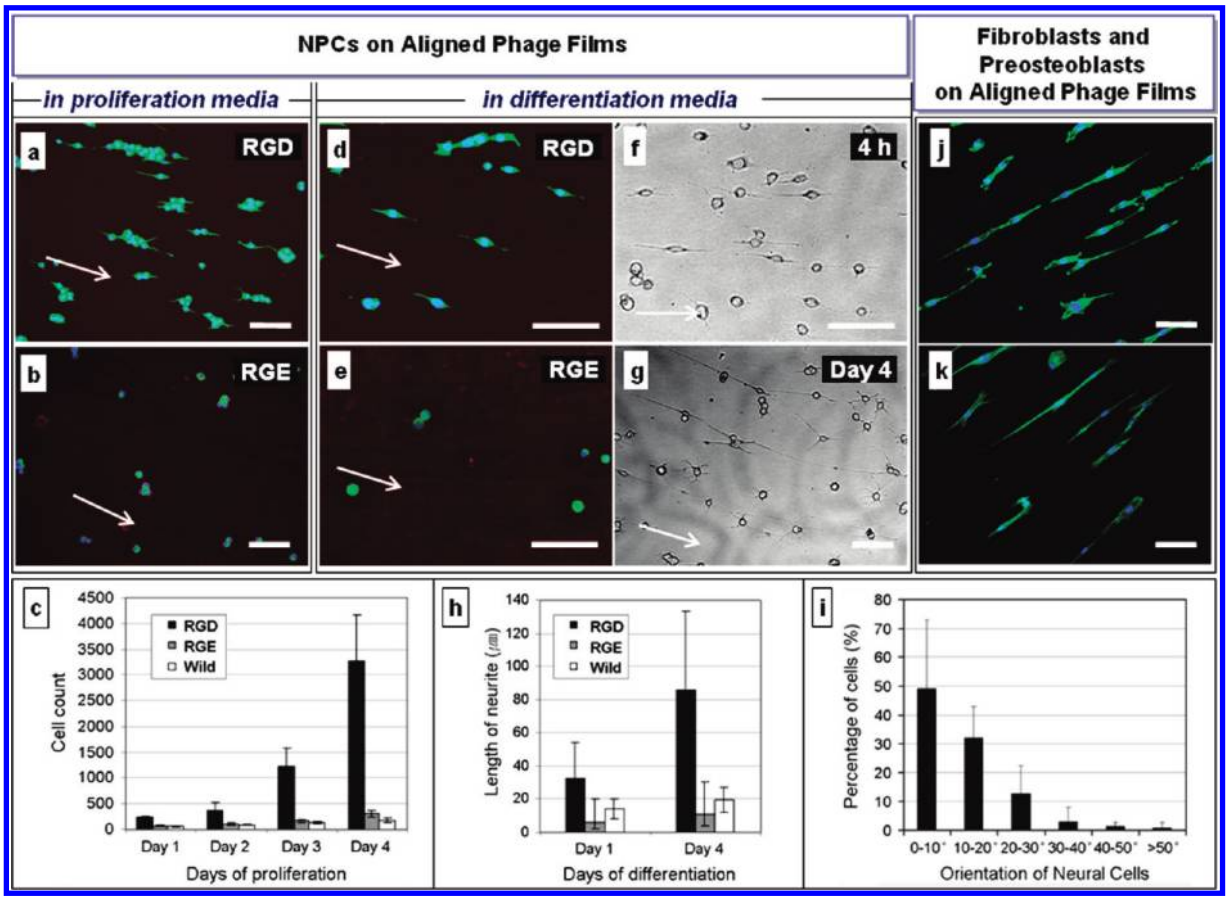

Figure 4. Effects of the aligned phage film on cell growth. Composite immunofluorescent staining images of NPCs grown on the (a) aligned RGD-phage film (day 1) and (b) aligned RGE-phage film (day 1) in a proliferation medium. (c) Counts of adhered NPCs on aligned phage films (days 1−4). Composite immunofluorescent staining images of NPCs grown on the (d) aligned RGD-phage film (day 1) and (e) aligned RGE-phage film (day 1) in a differentiation medium. Bright-field optical micrograph of NPCs on the aligned RGD-phage film at (f) 4 h and (g) day 4. (h) Neurite lengths of the differentiated NPCs on aligned phage films. (i) Distribution of neurite orientation grown on the aligned RGD-phage film (day 4). Composite fluorescence images of (j) NIH-3T3 fibroblasts and (k) MC-3T3-E1 preosteoblasts grown on the aligned RGD-phage (12 h). Actin fibers and nuclei were stained with phalloidin and DAPI, respectively. All scale bars indicate 100 μm.

the direction of phage fiber bundle alignment (Figure 4a). In contrast, because of poor cell adhesion, NPCs were neither flattened nor aligned within 1 day of culturing on the sheared RGE- and wild-type-phage films (elongation $\approx 1.1 \pm 0.1$) (Figure 4b, Supporting Information Figure S6a). On both the sheared and drop-cast control-phage films, the NPCs aggregated into neurospheres. Cell counts were taken on each phage film for 4 days, showing the effect of the RGD-phage films on increasing cell attachment and proliferation compared to that of the RGE- and wild-type-phage films (Figure 4c and Supporting Information Figure S6).

The ability of the aligned phage films to direct NPC differentiation was also examined. NPCs were seeded (3×10^4 cells/cm^2) on each aligned phage film (RGD, RGE, and wild-type) in the presence of differentiation media (Figure 4d−g and Supporting Information Figure S6). After 24 h, the cells on the aligned RGD phage film exhibited an outgrowth of neurites in a direction parallel to the phage alignment (Figure 4d). Differentiation into a neuronal lineage was verified by immunostaining of β-III-tubulin. In contrast, the NPCs on the aligned RGE- and wild-type-phage films appeared to be barely attached to the film surfaces and were mostly round in shape under the same condition (Figure 4e and Supporting Information Figure S6). When NPCs were observed for a prolonged time, they were found to adhere to the aligned RGD-phage film and exhibited spreading of their filaments within 4 h and continuously grew their neurites along the sheared direction for 4 days (Figure 4f,g). However, the NPCs on the aligned RGE- and wild-type-phage films were sparsely distributed with shorter processes and were not spread out on the substrates because of the absence of a cell-binding motif on the phage film (Supporting Information Figure S6). On RGD-phage films, differentiated NPCs cells elongated and their neurites grew faster (2−4 times on day 1) and extended further (4−7 times on day 4) than those of cells on the control-phage films (Figure 4h). The percentage of cells extending their neurites to within less than 20° of the direction of RGD-phage alignment was ~80% (Figure 4i). These results show the effects of biochemical and topographical cues from the aligned phage films in guiding directional cell growth. We also tested the ability of the aligned phage films to orient the growth of other cell types. When NIH-3T3 fibroblasts and MC-3T3-E1 preosteoblasts were cultured on aligned RGD-phage films (Figure 4j,k), their cytoskeletons and nuclei were elongated along the long axis of the aligned RGD-phage films.

Summary

We have developed genetically engineered liquid-crystalline viral films that can be used as tissue-engineering materials with the tunability of both topographical and biochemical properties. We genetically engineered M13 viruses to display integrin-binding RGD peptide motifs on their major coat proteins and self-assembled them into long-range-ordered films with anisotropic

topographies. We could tune the nanometer-scale topography and surface roughness of the viral films by varying the concentrations of the phage solution without having to use any microfabrication techniques. The resulting aligned viral structures with RGD motifs exhibited the ability to guide neural cell growth. The genetically incorporated RGD peptides on the phage played a pivotal role in inducing specific interactions between the films and the neural cells. Our virus-based tissue-regenerating materials may result in the development of future therapies for treating challenging medical conditions (e.g., spinal cord injuries) and serve as an in vitro model for studying complicated cell-signaling environments.

Acknowledgment. This work was supported by the Hellman Family Faculty Fund (S.-W.L.), start-up funds from the Nanoscience and Nanotechnology Institute at the University of California, Berkeley (S.-W.L.), the Laboratory Directed Research and Development Fund from the Lawrence Berkeley National Laboratory, a Korean Research Foundation grant funded by the Korean Government (MOEHRD) (KRF-2006-352-D00048), and a graduate student fellowship from the National Science Foundation (A.M.).

Supporting Information Available: Density calculation for peptides displayed on RGD-phage surfaces. Preparation of a laminin-coated surface (positive control) and cell plating. Composite immunofluorescent staining images of NPCs grown on the wild-type-phage film. Immunofluorescent staining images. Polarized optical micrographs of the liquid-crystalline solutions. Optical microscope images of NPCs cultured on aligned phage films and a laminin-coated substrate in a proliferation medium. Fluorescent images of NPCs grown on an aligned wild-type-phage film. Plot of the spatial distribution of differentiated NPCs on phage-coated substrates. This material is available free of charge via the Internet at http://pubs.acs.org.